

Fatigue and Static Performances of Butterfly Joints Under Hygrothermal Exposure Conditions

Gürkan Altan, Muzaffer Topçu

Faculty of Engineering, Department of Mechanical Engineering, Pamukkale University, Kınıklı 20070, Denizli, Turkey

Correspondence to: G. Altan (E-mail: gurkanaltan@pau.edu.tr)

ABSTRACT: In this study, the static and dynamic behaviors under different environmental conditions of mechanical insert butt joints with butterfly joint locks that could be used instead of adhesively bonded butt joints in composite plate joints were investigated. The experimental specimens and butterfly-shaped joining components with the same material configuration were cut from a $[(0/90)_8]_s$ laminated composite plate with a water jet in harmony with the geometric parameters. The fatigue experiments were carried out at a constant load ratio of 0.1 and at different maximum fatigue loads. To compare the joints with each other, the experiments were conducted under a 10-Hz fatigue frequency and under a tension–tension load with constant amplitude of a sinus curve shape. © 2012 Wiley Periodicals, Inc. *J. Appl. Polym. Sci.* 000: 000–000, 2012

KEYWORDS: composites; failure; fatigue analysis

Received 4 February 2011; accepted 5 January 2012; published online 00 Month 2012

DOI: 10.1002/app.36786

INTRODUCTION

Composite structures are usually jointed with mechanical joints or adhesives. Although industrial adhesives are used in bonded joints, joining components, such as bolts, pins, and rivets, are more commonly used in mechanical joints. It has been determined from studies on mechanical joints that joining regions are often exposed to such loadings as tension, shear, and bearing.¹ Composite structure joints can be bonded through different designs. Factors, such as the harmony of the adhesive with the composite material, type of the joint geometry, and bonding thickness, affect the load-carrying capacity.² The load-carrying behaviors of the joints made and their advantages or disadvantages over each other have been investigated numerically and experimentally by many researchers, and there are still studies being done in this field.

Kim et al.³ presented a methodology for the failure prediction of composite single-lap bonded joints considering both the composite adherent and the bondline failures. In this methodology, they used an elastic–perfectly plastic model of the adhesive and a delamination failure criterion. They verified their suggested technique with the numerical investigation. Goeij et al.⁴ evaluated which methods were used to determine the adhesive fatigue properties, the factors that influence the performance of a joint. Megueni et al.⁵ used the finite element method to analyze the evolution of the stress intensity factor for cracks

repaired with bonded hygrothermal aged composite patches. Sen et al.⁶ performed an experimental failure investigation to determine the failure mode and bearing strength of mechanically fastened bolted joints in glass-fiber-reinforced epoxy-laminated composite plates. El Mahi and Bezazi⁷ carried out an experimental work to determine the flexural behavior of two types of crossply laminates, glass-fiber/epoxy laminates and hybrid glass-fiber/Kevlar-fiber/epoxy laminates under fatigue load. Harman and Wang⁸ optimized the profile of the scarf joint between dissimilar modulus adherents with an analytical method. Chen⁹ examined the effects of hygrothermal cycling upon the performance of a bolted composite joint. He determined that the bolt torque relaxed as the number of environmental cycles increased. Avila and Bueno¹⁰ carried out a performance study on a new design of single-lap bonded joint, the so called wavy lap joint, for laminate composites. Topçu et al.¹¹ investigated the damage forces formed on glass-fiber-laminated composite plates that were jointed with a component in the shape of a butterfly with an experimental method. Choi and Chun¹² investigated a failure area method to predict the failure loads of mechanically fastened composite joints under plane stress conditions. Herrington and Sabbaghian¹³ investigated the effects of a number of parameters, the applied stress level, orientation of the outer-layer reinforcing filaments, and bolt torque level, on the fatigue life or the fatigue characteristics of a bolted graphite/epoxy composite laminate.

© 2012 Wiley Periodicals, Inc.

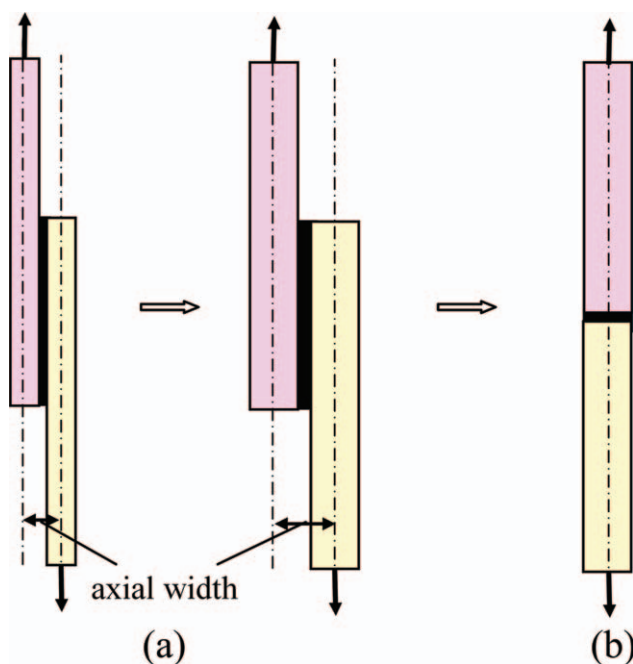


Figure 1. (a) Single lap joint with axial width and (b) butt joint without axial width. [Color figure can be viewed in the online issue, which is available at wileyonlinelibrary.com.]

The joint of composite materials is commonly made with mechanical or bonding techniques through a single or double lap. Particularly in single-lap bolted or bonded joints, an increase in the thickness of the composite structure negatively affects the strength of the whole jointed composite structure. In such joints, high stresses occur on the joint surface, and the strength of the structure is reduced with an increase in the axial width amount of the jointed composite plates.¹⁴ In other words, the load-carrying capacity is reduced with an increase in the axial width. Damage to the laminated structure plates joined through a single lap with adhesive usually occurs on the top layer.¹⁵ An increased axial width in mechanical joints leads to the damage of such joining components as the bolts, pins, and rivets.¹⁶ As shown in Figure 1, butt bonded joints are more commonly preferred, especially in thick composite structures. Because of the scarcity of design in butt joints, bonded joints are more often used instead of mechanical joints. In such joints, scarf or step joints are more often preferred over butt joints to prevent peeling stress.¹⁷ Even though the joint shapes are changed in bonded butt joints, peeling stress negatively affects the joint life-span. In this study, therefore, mechanical joints were used that could lock two plates face to face in shape without an adhesive.

In this study, we did not analyze bonded butt joints but instead made mechanical butt joints with butterfly-shaped joining components; these are usually used in the furniture industry and have not been used in composite structures before according to a literature review. The experiments were done with specimens cut out from the composite plate, which was mechanically joined face to face, as shown in Figure 2. All experimental specimens and butterfly-shaped joining components with the same

material configuration were cut from manufactured $[(0/90)_8]_s$ laminated composite plates. The butterfly-shaped joining components were used in mechanical butt joints with a tight insertion method to join the composite plates face to face. The effects of changes in the geometric parameters of the butterfly-shaped joining components (x/w , y/b , and w/b), as shown in Figure 2, on the maximum load-carrying capacity were analyzed by Altan in his doctoral study,¹⁸ and the best joint geometries were found to be at ratios of $x/w = 0.2$, $y/b = 0.4$, and $w/b = 0.4$. Here (w) is the end width, (x) is the middle width and (y) is the half length of the joint lock in the shape of butterfly. The butterfly-shaped joining components used in this study were selected under these geometric ratios, under which the best strength values were obtained according to the optimization experimental data of Altan and with a 0.05-mm tight insertion clearance. Henkel Loctite 9464, which is applied like paste, was used as the adhesive. The moisture and water absorption effects of the butterfly joints were analyzed, and their static/fatigue performances were investigated under different conditions. The fatigue performances of the butterfly joints were analyzed with and without adhesive at, below, and above room temperature.

MECHANICAL PROPERTIES OF THE COMPOSITE MATERIAL

The density of the composite plate (ρ_K) was found first by determination of the volume ratios of the glass fiber–epoxy composite plate produced with the hot-pressing method. For this purpose, the glass fibers used as fiber materials before the production of the composite plate were weighed. The weight of the matrix material was calculated by subtraction of the weight of the fiber material from the total weight of the produced composite plate. The weight of the total composite plate was measured as 3600 g, and the weight of the glass fibers was 2160 g. The densities (ρ 's) of the matrix and fiber were obtained from eq. (1), and their volume ratios were obtained from eqs. (2) and (3):

$$\rho = \frac{m}{V} \quad (1)$$

$$V_f(\%) = \frac{V_f}{V_T} \times 100 \quad (2)$$

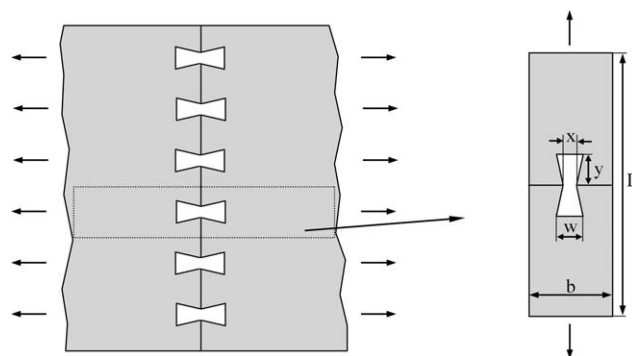


Figure 2. Mechanic butt joint with the butterfly joining component. Here (L) is the specimen total length.



Figure 3. Experiment with the video extensometer. [Color figure can be viewed in the online issue, which is available at wileyonlinelibrary.com.]

where V_f is volume ratio of glass fibers in the composite material, V_m is volume ratio of the matrix in the composite material and V_T is total volume ratio of the matrix and fiber in the composite material.

$$V_m(\%) = \frac{V_m}{V_T} \times 100 \quad (3)$$

The volume ratio of glass fibers in the composite material was $V_f = 0.59$, and the volume ratio of the matrix was $V_m = 0.41$. In this case, ρ_K was found to be 2.026 g/cm^3 from eq. (4):

$$\rho_K = V_f \rho_f + V_m \rho_m \quad (4)$$

where ρ_f is density of the fiber in the composite material and ρ_m is volume ratio of the matrix in the composite material.

The mechanical properties of glass fiber–epoxy composite materials have been determined according to ASTM standards under the loads of tension, compression, and shear.^{19–23} Because the composite plate was made from unidirectional glass-fiber cloths, the mechanical properties varied in two different directions. Its direction parallel to the fiber (1) was accepted as the direction perpendicular to the fiber (2). The mechanical properties of the composite plate on surfaces 1 and 2 were obtained with three specimens for each mechanical property, and the average properties were obtained.

The experiments made for the determination of the mechanical properties were carried out under ASTM standards at $23 \pm 1^\circ\text{C}$ (room temperature) and $50 \pm 10\%$ relative humidity. The experiments were done with an Instron 8801 instrument with a capacity of a 50-kN load. The strains were determined with a

Table I. Mechanical Properties of the Composite Material

E_1 (MPa)	E_2 (MPa)	G_{12} (MPa)	X_t v_{12}	Y_t (MPa)	X_c (MPa)	Y_c (MPa)	S (MPa)
44,150	12,300	4096	0.20	775	130	305	80

v_{12} , Poisson ratio; E_1 , longitudinal modulus; E_2 , transverse modulus.

two-way video extensometer, as shown in Figure 3. The video extensometer could determine the strains without any need to stick a strain gauge on the surface of the specimens and without touching. Some points were marked in the directions of 1 and 2 on the specimen with a special marking pen, and we could determine how much the distance between these points was elongated or shortened during the experiment with the aid of the video extensometer. The amount of the determined elongation or shortening helped to determine the amounts of strain belonging to those directions of the material.

The mechanical properties of the composite material obtained under room conditions are given in Table I.¹⁸

Effects of the Temperature and Humidity on the Mechanical Properties

It may be said that temperature and humidity are the primary factors that affect the mechanical properties of fiber–epoxy composite materials. This study was devoted to the analysis of the temperature- and humidity-based changes in the mechanical properties of the composite materials reinforced with glass fibers. Enabling different temperature and humidity conditions, a climatic cabinet hosted the tension experiments made according to ASTM standards. Here, the changes in the elasticity modulus in the tension direction of 1 of the composite materials at different temperature and humidity ratios were taken into consideration. The changes in the temperature and humidity effects were obtained with at least three specimens, and then, the average values were obtained. The experiments on the specimens were carried out after they were kept for 24 h under different temperatures and humidity conditions. Figure 4 shows the changes of the average elasticity modulus of the composite materials exposed to the same humidity conditions at and above room temperature. The experiments were conducted at $50 \pm 5\%$ relative humidity (room conditions) and $90 \pm 5\%$ relative humidity (humid condition). We determined from the experiments made at room temperature and two different humidity conditions that the elasticity modulus obtained in the humid condition was 1% lower than the elasticity modulus obtained under the room condition. At temperatures above room temperature, however, this reduction was found to be around 1.4%.

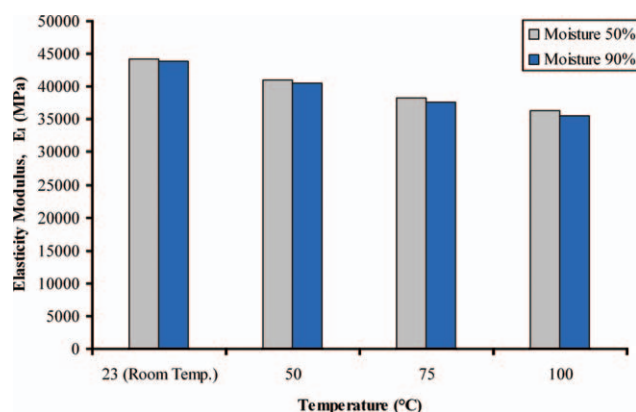


Figure 4. Changes in the elasticity modulus at and above room temperature. [Color figure can be viewed in the online issue, which is available at wileyonlinelibrary.com.]

Table II. Mechanical Properties at and below Room Temperature

Temperature (°C)	E_1 (MPa)	ν_{12}
-20	45,500	0.21
23 (room temperature)	44,150	0.20

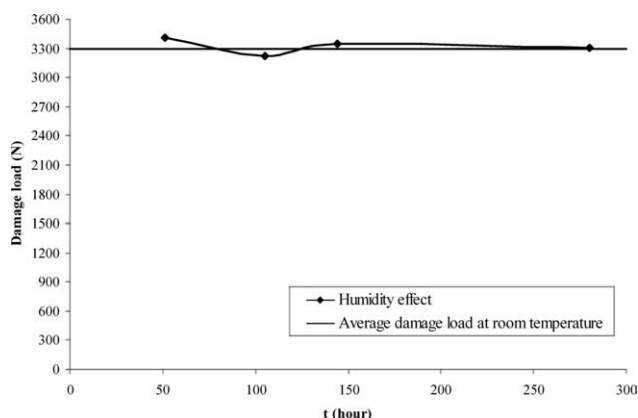
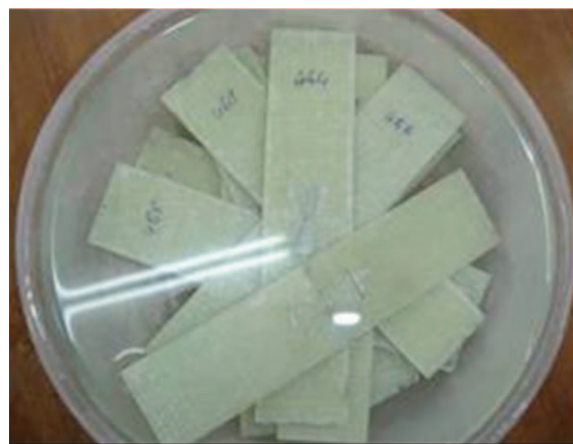
E_1 , elasticity modulus; ν_{12} , Poisson ratio.

As shown in the figure, we determined that when the temperature rose from room temperature to 100°C in the humid condition, the elasticity modulus fell by around 18.9%. We also found out from the experiment's results that when the humidity of the environment was around 50% and there was the same increase in temperature, this fall was around 17.9%. It was obvious from these results that the humidity did not have an extreme effect on the mechanical properties, but the mechanical properties changed much more with the increase in temperature.

The mechanical properties obtained at and below room temperature are given in Table II. Accordingly, the elasticity modulus obtained at -20°C is higher than the elasticity modulus obtained at room temperature.

HUMIDITY EFFECT ON THE BUTTERFLY JOINTS

The humidity effect on the butterfly joints was analyzed for the joints with adhesive on the butterfly joining component. The composite layer numbers of the specimens and butterfly joining components were taken as 16, and their fiber orientation angles were taken as 0/90°. Loctite 9464 was used as the adhesive. In this section of the study, at least three samples were used for each value. The change in the effect of humidity on the damage loads of the bonded butterfly joints is shown in Figure 5. Here, the terms of damage load used were characterized by the strength of butterfly joints. In other words, the *damage load* could be defined as the maximum load immediately before failure of the butterfly joints. The experiments of the specimens were carried out at 90% relative humidity for 280 h. All of the experiments were also conducted at room temperature. As shown in Figure 5, we determined that the damage load values obtained at different waiting periods and in the humid condition were equal to the average damage load value obtained in the room condition. Primarily, separations at the joining zone

**Figure 5.** Change of the damage loads at 90% relative humidity. t , time (hour).**Figure 6.** Water absorption properties of the specimens. [Color figure can be viewed in the online issue, which is available at wileyonlinelibrary.com.]

were observed as a type of damage on flat surfaces. After this first type of damage, when the loading was continued, we observed that the butterfly-shaped joining components suffered damage. Although the specimens were kept in a humid environment for almost 12 days, the humidity, namely, the water due to humidity, was not absorbed by the composite material. Thus, we found out that the specimens kept in a humid environment were not affected by the humidity or that its effect was negligible.

WATER ABSORPTION PROPERTIES OF THE BUTTERFLY JOINTS

To analyze the water absorption properties of the tightly inserted butterfly joints, the experimental specimens were kept in a water-filled bowl for 192 h, as shown in Figure 6. The experiments were carried out in the room condition. To determine the water absorption properties of the specimens, the butterfly joining components were applied, but no adhesive was used.

In this way, we ensured that all of the surfaces of both the butterfly joining components and the specimens remain under the effect of water. As the bottom and top surfaces of the composite specimen materials were covered with epoxy during manufacturing, water was not been absorbed through these surfaces. Because the specimens and butterfly joining components were cut out from composite plates, the epoxy layer covering the border surfaces was eliminated. The absorption of water by the specimen was gradually caused by the glass-fiber sections seen on the border surfaces due to cutting. The water absorption of the specimens was possible through the gaps that appeared around the glass fibers and with the settlement of this water mass on the interface between the glass fibers and the matrix. The amount of water on the interface between the glass fibers and the matrix exhibited a cushion effect and influenced the strengths of the specimens. The specimens were loaded up to failure, and then, each damage load was obtained. The effects of the water absorption properties of the specimens on the damage loads are shown in Figure 7. Each damage load obtained was the average of the three experiments. As shown in the figure, as the amount of absorbed water increased over time, the damage

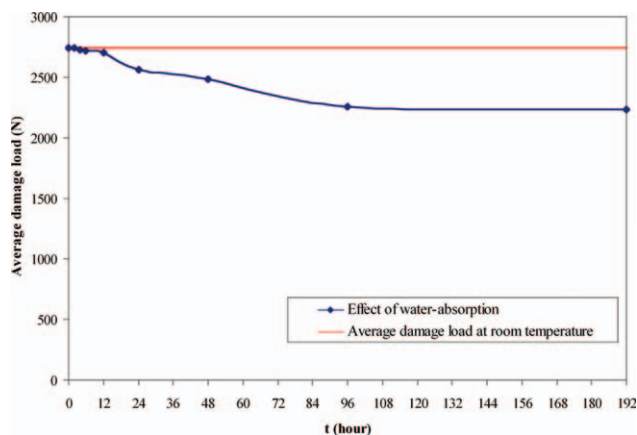


Figure 7. Effects of the water absorption of the butterfly joints. t , time (hour) [Color figure can be viewed in the online issue, which is available at wileyonlinelibrary.com.]

load values decreased gradually. However, after the slice of time when the water absorption was almost equal, namely, 96 h, the damage load values were discovered to remain at the same level.

EFFECT OF THE TEMPERATURE ON THE DAMAGE LOADS IN THE BUTTERFLY JOINTS

In this part, the tightly inserted and bonded butterfly joints with the $[(0/90)_8]_s$ composite material are considered. The maximum damage load values of these two types of butterfly joints above room temperature were analyzed. As shown in Figure 8, static experiments conducted above and below the room temperature were made in a climatic cabinet containing tension jaws. As shown later in Figure 16(b), the static experiments made below room temperature were in an insulated climatic cabinet cooled with CO_2 gas. Each experimental datum obtained was the average of the same three experiments. The experiments were conducted after the specimens were kept at the same temperature at least for 2 h. To compare the experimental data obtained, the experiments were all carried out at the same tension velocity (1 mm/min).

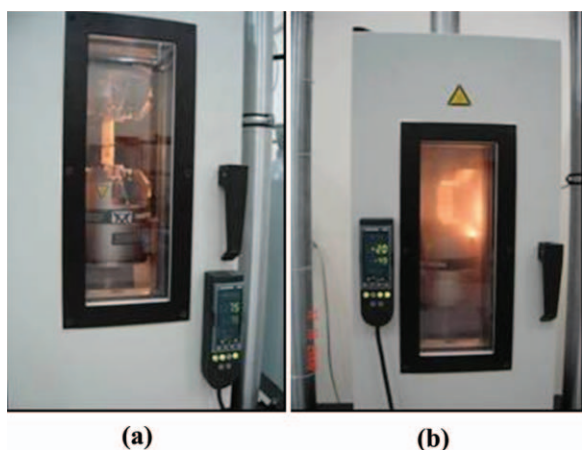


Figure 8. Static experiments conducted (a) above and (b) below room temperature. [Color figure can be viewed in the online issue, which is available at wileyonlinelibrary.com.]

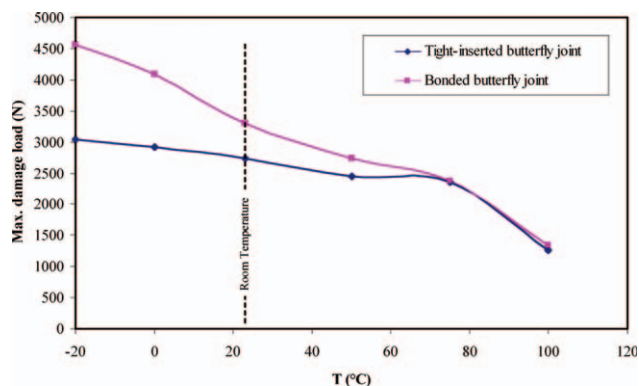


Figure 9. Changes in the damage loads of the butterfly joints under temperature (T) effect. [Color figure can be viewed in the online issue, which is available at wileyonlinelibrary.com.]

The changes in the damage loads of the butterfly specimens joined at different temperatures are given in Figure 9. The static damage load of the tightly inserted butterfly joints was 2740 N at room temperature, and the static damage load of the bonded butterfly joints was 3300 N at room temperature. As shown in the figure, the damage load values decreased with increasing temperature. We determined that the damage load reduction that occurred with the increase in temperature in the tightly inserted butterfly joints was lower than the damage load reductions in the bonded butterfly joints. The adhesion process was carried out on the surfaces of the specimen thickness at the joining zone. Because of the effect of the adhesive on the bonded butterfly joints, a high damage load reduction occurred. We observed from the experiments conducted above room temperature that the process of locking on the joining regions of the specimens, due to the softening of the matrix material, weakened them, or in other words, the inclined arm parts of the specimens holding the butterfly joining components opened more widely. Hence, the experimental data affirmed that the load-carrying capacities of the joint were reduced. Because of the fact that the matrix material was harder at temperatures below room temperature than at temperatures above room



Figure 10. Fatigue test in the climatic cabinet. [Color figure can be viewed in the online issue, which is available at wileyonlinelibrary.com.]

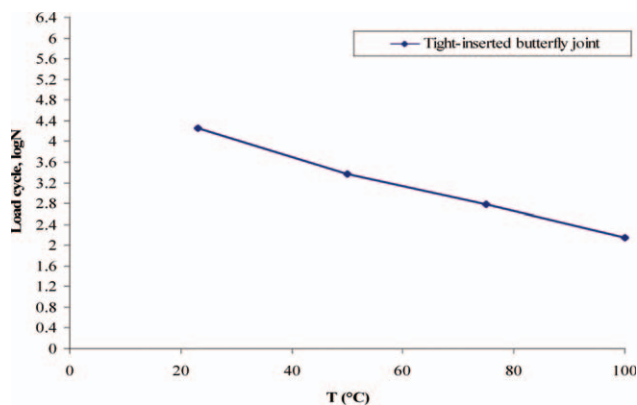


Figure 11. Changes in the fatigue performances of the butterfly joint without adhesive exposed to different temperatures (T 's = temperatures). N , Load cycle [Color figure can be viewed in the online issue, which is available at wileyonlinelibrary.com.]

temperature, we found out that the inclined arm parts of the specimens held the butterfly joining components more tightly; that is, the process of locking was stronger. As shown in Figure 9, the load-carrying capacities increased more under the effect of the adhesive at temperatures below room temperature.

FATIGUE PERFORMANCES OF THE BUTTERFLY JOINTS AT DIFFERENT TEMPERATURES

The fatigue performances of the butterfly joints were analyzed only at different temperatures because the effect of the humidity on the mechanical properties was negligible, as inferred from the experiments. The fatigue experiments were carried out at a constant load ratio of 0.1. To compare the joints with each other, the experiments were conducted under a 10-Hz fatigue frequency and a tension–tension load with a constant amplitude of a sinus curve shape. The fatigue performances of the butterfly joints were analyzed in a climatic cabinet, as shown in Figure 10. To obtain temperatures above room temperature, the climatic cabinet was heated with resistances and controlled with a digital control unit. For temperatures below room temperature,

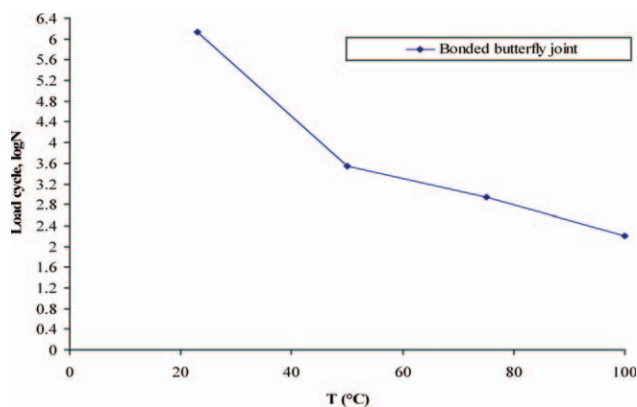


Figure 12. Changes in the fatigue performances of the butterfly joint with adhesive exposed to different temperatures (T 's = temperatures). N , Load cycle. [Color figure can be viewed in the online issue, which is available at wileyonlinelibrary.com.]

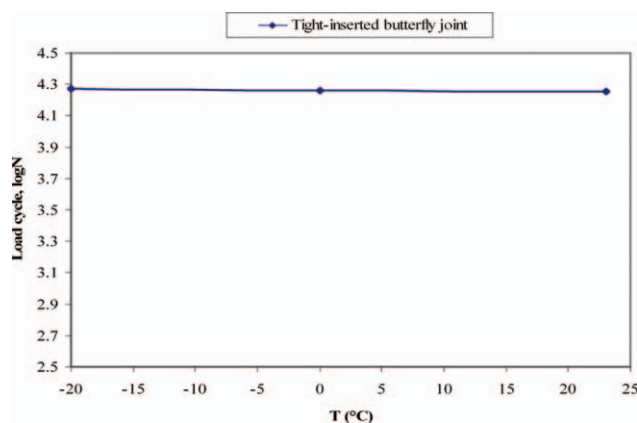


Figure 13. Changes in the fatigue performances of the butterfly joint without adhesive exposed to different temperatures (T 's = temperatures). N , Load cycle. [Color figure can be viewed in the online issue, which is available at wileyonlinelibrary.com.]

the climatic cabinet was cooled with CO_2 gas. Fatigue experiments were carried out with at least three specimens, and the average values of the experimental values were taken. To analyze the changes in fatigue performance under different temperatures, experimental temperature values of 50, 75, and 100°C were used. Here, the number of load cycles obtained shows the damage life at various temperatures. The experiments were done at 50% relative humidity. The specimens were kept for at least for 2 h at the temperature values under which the experiment was conducted.

To determine the effect of temperature in the fatigue performances of the tightly inserted butterfly joints, the maximum fatigue loads of the tightly inserted butterfly joints, the average damage load of which was fixed as 2740 N, were taken to be around 60% of the static value. Figure 11 shows the changes in the average load cycles obtained, which depended on the temperature values. As shown in the figure, the highest load cycles were obtained at room temperature. Parallel to the reductions in strength obtained from the static experiments conducted at

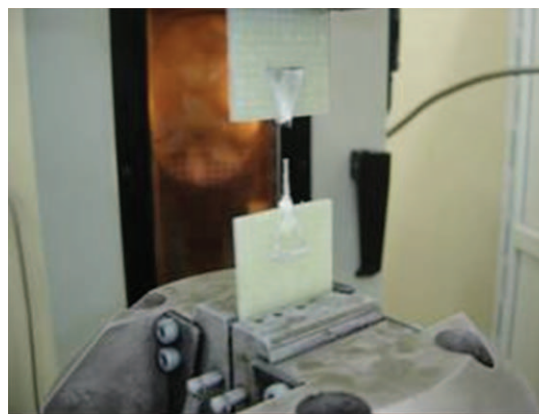


Figure 14. Fatigue damage shapes of the butterfly joints without adhesive. [Color figure can be viewed in the online issue, which is available at wileyonlinelibrary.com.]

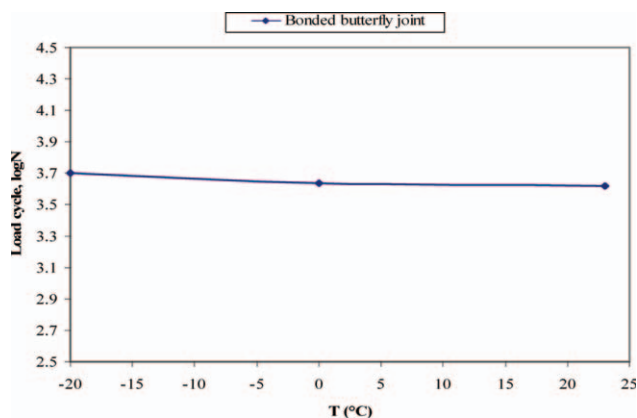


Figure 15. Changes in the fatigue performances of the butterfly joint with adhesive exposed to different temperatures (T 's = temperatures). N, Load cycle. [Color figure can be viewed in the online issue, which is available at wileyonlinelibrary.com.]

temperature values above room temperature, reductions were observed in the load cycles in the fatigue experiments. The reductions that occurred in the load cycles at high temperatures appeared to have stemmed from the fact that the arm parts of the specimens holding the butterfly joining components bent more because they became softer.

The maximum fatigue loads of the bonded and inserted butterfly joints, the average damage load of which was fixed as 3300 N, were taken to be around 50% of the static value. As shown in Figure 12, the highest load cycles were obtained from the fatigue experiments conducted at room temperature. Because the fatigue average and amplitude load values of the butterfly joints were equal to the load values of the tightly inserted butterfly joints, we determined that the load cycles obtained from the butterfly joints bonded at each temperature were generally higher when they were compared with each other. We also found out that the fatigue load cycles of the bonded butterfly joints were 75 times higher than those of the tightly inserted

butterfly joints at room temperature and around 1.5 times higher at temperature values above room temperature.

At least three specimens were used in the fatigue experiments in a cold environment, and the average values of the experimental data were taken. To analyze the changes in fatigue performance under cold conditions, experimental temperature values of 0 and -20°C were used. The specimens were kept for at least for 2 h at the temperature value under which the experiment was conducted. Then, the fatigue performance of each specimen was investigated. To analyze the fatigue performances of the tightly inserted butterfly joints at temperature values below room temperature, the maximum fatigue loads were taken to be around 60% of the average static tension value. Figure 13 shows the temperature-based changes in the fatigue load cycles obtained from the fatigue experiments conducted at -20 and 23°C . As shown in the figure, the highest load cycles were obtained at -20°C . Parallel to the increases in the damage load obtained from the static experiments conducted at temperature values below room temperature, increases were observed in the load cycles in the fatigue experiments as well. The increases in the load cycles at lower temperatures may have been due to the stiffening of the matrix material of the composite specimen. The load cycle obtained at -20°C was found to be 5% higher than the load cycle obtained at room temperature.

Figure 14 contains a sample picture of the fatigue damage and shows the fatigue damage shapes of the tightly inserted butterfly joints under cold conditions. The fatigue damages of the butterfly joints at all temperature values were determined to always occur on the butterfly midwidth.

The maximum fatigue loads of the bonded butterfly joints were taken to be around 80% of the average damage load value. As shown in Figure 15, the highest load cycles were obtained from the fatigue experiments at -20°C . The fatigue load cycle obtained at -20°C was determined to be 20% higher than the load cycle obtained at room temperature. An increase in the fatigue load cycles was obtained with the effect of the adhesive.

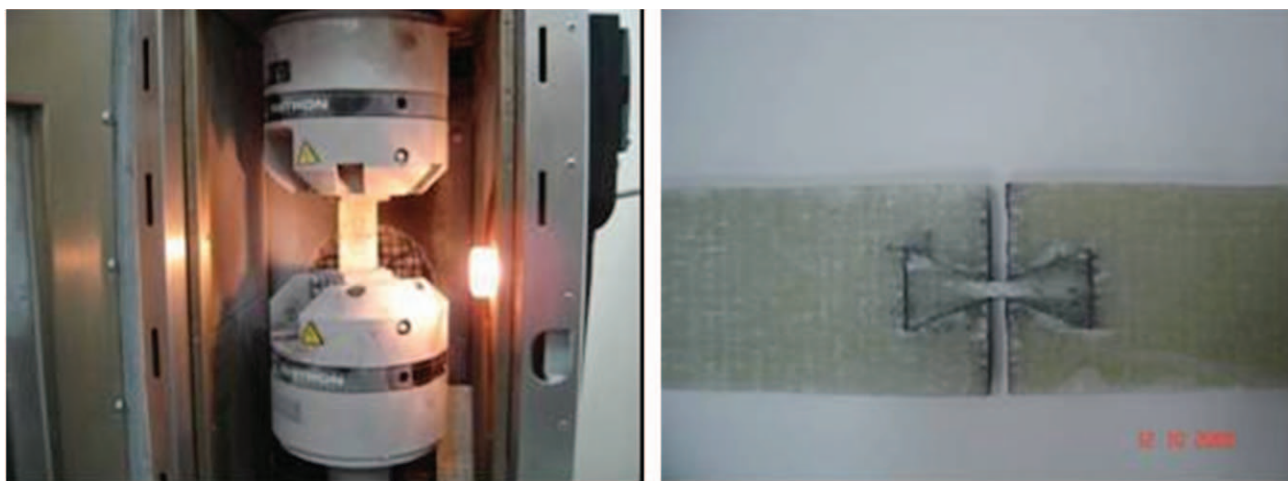


Figure 16. Fatigue damage shapes of the butterfly joints with adhesive. [Color figure can be viewed in the online issue, which is available at wileyonlinelibrary.com.]

Sample pictures of the fatigue damage shapes of the bonded butterfly joints under cold conditions are given in Figure 16. As shown in the figure, the flat surfaces that were bonded first were broken, leaving the butterfly midwidth exposed to fatigue load.

CONCLUSIONS

The static and fatigue performances of butterfly-shaped joints under different temperatures and humidities were analyzed experimentally in this study. The glass fiber–epoxy composite material used in the experiments was produced with the hot-pressing method. The following are the conclusions we derived from this study:

- The fatigue performances of the bonded butterfly joints were much better than those of the others. As the specimens joined in the butterfly joints reinforced with the adhesive worked mechanically and as a bonded joints, their fatigue performances were found to be as very high. At the same time, the bonded surfaces were increased more and more in the bonded butterfly joints than in other joints, such as butt joints.
- In the joints in which there was only tight insertion, fatigue damages occurred only in the butterfly midwidth, and therefore, their lifespan of fatigue was found to be rather short.
- Humidity experiments with the butterfly joints were conducted at 90% relative humidity, under which they were kept for as long as 280 h. We determined that they were not affected by the humidity or that this effect was negligible.
- The load-carrying values of the butterfly joints immersed in water diminished a little under the effect of the water mass placed in the interface between the glass fibers and matrix.
- Generally, with an increase in temperature in the butterfly joints, both the static and fatigue strength values were found to fall. However, these values were determined to increase at temperatures below room temperature.

ACKNOWLEDGMENTS

The authors would like to express their appreciation to the TUBITAK, Turkey, Project No: 106M113 for providing financial support for this study.

REFERENCES

1. Karakuzu, R.; Gülem, T.; İçten, B. M. *Compos. Struct.* **2006**, *72*, 27.
2. Silva, L. F. M.; Adams, R. D. *Int. J. Adhes. Adhes.* **2007**, *27*, 362.
3. Kim, K. S.; Yi, Y. M.; Cho, G. R.; Kim, C. G. *Compos. Struct.* **2008**, *82*, 513.
4. Goeij, W. C.; Tooren, M. J. L.; Beukers, A. *Mater. Des.* **1999**, *20*, 213.
5. Megueni, A.; Tounsi, A.; Adda Bedia, E. *Mater. Des.* **2007**, *28*, 287.
6. Sen, F.; Pakdil, M.; Sayman, O.; Benli, S. *Mater. Des.* **2008**, *29*, 1159.
7. El Mahi, A.; Bezazi, A. *Appl. Compos. Mater.* **2009**, *16*, 33.
8. Harman, A. B.; Wang, C. H. *Compos. Struct.* **2008**, *75*, 132.
9. Chen, H. S. *Compos. Struct.* **2001**, *52*, 295.
10. Avila, F. A.; Bueno, P. O. *Compos. Struct.* **2004**, *64*, 531.
11. Topçu, M.; Altan, G.; Ergun, E. *Adv. Compos. Lett.* **2007**, *16*, 197.
12. Choi, J. H.; Chun, Y. J. *J. Compos. Mater.* **2003**, *37*, 2163.
13. Herrington, P. D.; Sabbaghian, M. J. *Compos. Mater.* **1993**, *27*, 491.
14. Gunnion, A. J.; Herszberg, I. *Compos. Struct.* **2006**, *75*, 364.
15. Kinloch, A. J. *Adhesion and Adhesives*; Cambridge University Press: London, **1987**; p 441.
16. Mallick, P. K. *Fiber-Reinforced Composites*; Marcel Dekker: New York, **1993**; p 566.
17. Silva, L. F. M.; Adams, R. D. *Int. J. Adhes. Adhes.* **2007**, *27*, 362.
18. Altan, G. Ph.D. Thesis, Pamukkale University, **2009**.
19. Standard Test Method for Tensile Properties of Polymer Matrix Composite Materials; ASTM D 3039/D 3039M-00; American Institute of Testing and Materials: West Conshohocken, PA, **1979**.
20. Standard Test Method for Compressive Properties of Unidirectional or Crossply Fiber–Resin Composites; ASTM D 3410-75; American Institute of Testing and Materials: West Conshohocken, PA, **1979**.
21. Standard Recommended Practice for In Plane Shear Stress–Strain Response of Unidirectional Reinforced Plastics; ASTM D 3518–76; American Institute of Testing and Materials: West Conshohocken, PA, **1976**.
22. Jones, R. M. *Mechanics of Composite Materials*; Taylor & Francis: Philadelphia, **1999**; p 519.
23. Standard Test Method for Shear Properties of Composite Materials by the V-Notched Beam Method; ASTM D 5379/D 5379M-98; American Institute of Testing and Materials: West Conshohocken, PA, **1998**.